Estimation of failure probability function and its bounds under random and interval variables: A fully decoupled approach using Bayesian active learning

Jinxing Liu
PhD student, Inst. for Risk and Reliability, Leibniz Univ. Hannover, Hannover, Germany

Chao Dang
PhD student, Inst. for Risk and Reliability, Leibniz Univ. Hannover, Hannover, Germany
E-mail: chao.dang@irz.uni-hannover.de (corresponding author)

Matthias G.R. Faes
Prof., Chair for Reliability Engineering, TU Dortmund University, Dortmund, Germany

Marcos A. Valdebenito
Chief engineer, Chair for Reliability Engineering, TU Dortmund University, Dortmund, Germany

Michael Beer
Prof., Inst. for Risk and Reliability, Leibniz Univ. Hannover, Hannover, Germany

ABSTRACT: Random and interval variables can coexist in a single structural reliability analysis problem. The existing methods for such hybrid reliability analysis, however, cannot balance the computational cost and accuracy well. In this paper, a fully decoupled approach based on Bayesian active learning is developed to estimate the failure probability function (FPF) and its lower and upper bounds. First, the problem of estimating the FPF is turned into a Bayesian inference problem. A Gaussian process prior is assigned over the performance function, and conditional on observations the posterior expectation function and an upper bound of the posterior variance function of the FPF are derived. The posterior expectation can be naturally used as a FPF estimate, while the upper bound of the posterior variance measures our maximum epistemic uncertainty about estimate. Second, based on the uncertainty representation of the FPF, a two-stage strategy is proposed to select new points to enable efficient active learning. In the first stage, a global uncertainty contribution (GUC) function is devised to improve the global accuracy of the FPF estimate. In the second stage, to further reduce the local approximation error, a local uncertainty contribution (LUC) function is introduced. Third, the sequential Monte Carlo method is employed to deal with analytically intractable integrals. An example is studied to demonstrate the performance of the proposed approach.

1. Introduction

Various uncertainties associated with material properties, geometry dimensions, manufacturing imprecision, etc., can appear in engineering practice. Generally, uncertainties are classified into aleatory and epistemic (Helton and Burmaster (1996); Der Kiureghian and Ditlevsen (2009); Beer et al. (2013a)). Aleatory uncertainty describes inherent randomness which is irreducible, and random variables with precise probability distributions are used to characterize the uncertainty. Epistemic uncertainty exists subjectively due to the incomplete information, and can be quantified by non-probability models (Hong et al. (2021)), such as convex model (Luo et al. (2009)), fuzzy sets (Beer et al. (2013b)), and evidence theory (Jiang et al. (2013)). The aleatory and epistemic uncertainties usually coexist in engineering practice, which gives rise to hybrid problems. The resulting hybrid reliability analysis (HRA) is a challenge because the failure probability in this case is not a crisp value. In this paper, the variables with epistemic uncertainties are represented by interval variables, of which only intervals of variations are known.

For HRA with random and interval variables (HRA-RI), some methods have been developed. Although the double-loop Monte Carlo Simulation (MCS) can produce reliable results, it is not applicable due to its expensive computational costs. Unified uncertainty analysis (UUA) method based on the first order reliability method (FORM), known as FORM-UUA (X. Du (2008)), can calculate the bounds of failure probability efficiently. Besides, based on mean value first order saddle-point approximation (MVFOSA) method (Huang and Du (2008)), MVFOSPA-UUA (Xiao et al. (2012)) method is proposed to estimate the systems probabilities of failure considering random and interval variables simultaneously. Resorting to active learning Kriging (ALK) model, ALK-HRA (Yang et al. (2015)) is proposed to accurately estimate the lower and upper bounds of failure probability. To perform HRA-RI for complex systems, a sequential strategy combining subset simulation (SS) and Kriging is proposed (Brevault et al. (2016)), where a modification of the generalized max–min (GMM) is introduced to refine Kriging. Zhang et al. (2018) propose a new method combining a projection outline based active learning (POAL) and Kriging (POAL-Kriging), where the accuracy of projection outlines on the limit-state surface is proved to be crucial for HRA-RI.

Though those methods demonstrate effectiveness in HRA-RI, they have limitations regarding efficiency and/or accuracy. This paper aims to develop a novel fully decoupled approach dealing with HRA-RI based on the active learning probabilistic integration (ALPI) method presented in (Dang et al. (2021)). The proposed approach extends the application of the original ALPI to HRA-RI, whereas ALPI is only applicable in probabilistic reliability analysis. Different from double-loop simulation methods, the failure probability function (FPF) of interval variables is derived, of which the lower and upper bounds are identified efficiently in this method. First, a Bayesian framework is developed to perform Bayesian inference about the FPF. Second, based on the uncertainty representation of FPF, a two-stage experimental design is proposed to enable efficient active learning.

This paper is outlined as follows. Section 2 introduces the HRA-RI. In Section 3, the proposed fully decoupled method is elaborated. One numerical example is employed to test the performance of the proposed method in Section 4. Conclusions are given in Section 5.

2. HYBRID RELIABILITY ANALYSIS WITH RANDOM AND INTERVAL VARIABLES

For reliability analysis with random variables, the classical probabilistic method can be employed to calculate the structural failure probability, which is defined as:

$$P_f = \Pr\{G(\boldsymbol{X}) \leq 0\} = \iint \dots \int_{(G\leq 0)} f_{\boldsymbol{X}}(\boldsymbol{x}) d\boldsymbol{x}, \tag{1}$$

where $G(\boldsymbol{X})$ denotes the performance function, $\boldsymbol{X} = [X_1, X_2, ..., X_{n_{\boldsymbol{X}}}]^{\mathrm{T}}$ denotes the vector of random variables with precise distributions, $n_{\boldsymbol{X}}$ is the dimension of $\boldsymbol{X}$, and $f_{\boldsymbol{X}}(\cdot)$ is the joint probability density function (PDF) of $\boldsymbol{X}$.

For HRA-RI, however, the performance function is described as $G(\boldsymbol{X}, \boldsymbol{y})$. $\boldsymbol{y} = [y_1, y_2, ..., y_{n_{\boldsymbol{y}}}]^{\mathrm{T}} \in [\boldsymbol{y}^L, \boldsymbol{y}^U]$ represents the $n_{\boldsymbol{Y}}$-dimensional vector of interval variables, where $\boldsymbol{y}^L = [y_1^L, y_2^L, ..., y_{n_{\boldsymbol{y}}}^L]^{\mathrm{T}}$ and $\boldsymbol{y}^U = [y_1^U, y_2^U, ..., y_{n_{\boldsymbol{y}}}^U]^{\mathrm{T}}$ are vectors containing lower and upper bounds of $n_{\boldsymbol{y}}$ interval variables. In this case, the failure probability P_f is an interval rather than a crisp value. Under this setting, the bounds of failure probability are defined as (X. Du (2008)):

$$P_f^{max} = \Pr\left\{ \min_{\boldsymbol{y}^L \leq \boldsymbol{y} \leq \boldsymbol{y}^U} G(\boldsymbol{X}, \boldsymbol{y}) \leq 0 \right\}, \tag{2}$$

$$P_f^{min} = \Pr\left\{\max_{\boldsymbol{y}^L \le \boldsymbol{y} \le \boldsymbol{y}^U} G(\boldsymbol{X}, \boldsymbol{y}) \le 0\right\}, \tag{3}$$

where P_f^{max} is the upper bound of P_f, P_f^{min} is the lower bound of P_f, $\min G(\boldsymbol{x},\boldsymbol{y})$ and $\max G(\boldsymbol{x},\boldsymbol{y})$ are the minimum and maximum responses of performance function in terms of interval variables. Moreover, P_f^{max} and P_f^{min} in Eqs. (2) and (3) can be calculated by (Yang et al. (2015)):

$$P_f^{max} = \iint \dots \int I_F^U(\boldsymbol{x}) f_{\boldsymbol{X}}(\boldsymbol{x}) d\boldsymbol{x}, \tag{4}$$

$$P_f^{min} = \iint \dots \int I_F^L(\boldsymbol{x}) f_{\boldsymbol{X}}(\boldsymbol{x}) d\boldsymbol{x}, \tag{5}$$

where $I_F^U(\cdot)$ and $I_F^L(\cdot)$ are the failure indicator functions for the minimum and maximum responses of $G(\boldsymbol{x},\boldsymbol{y})$, defined as follows:

$$I_F^U(\boldsymbol{x}) = \begin{cases} 1, & \min\limits_{\boldsymbol{y}} G(\boldsymbol{x},\boldsymbol{y}) \le 0 \\ 0 & \min\limits_{\boldsymbol{y}} G(\boldsymbol{x},\boldsymbol{y}) > 0 \end{cases}, \tag{6}$$

$$I_F^L(\boldsymbol{x}) = \begin{cases} 1, & \max\limits_{\boldsymbol{y}} G(\boldsymbol{x},\boldsymbol{y}) \le 0 \\ 0 & \max\limits_{\boldsymbol{y}} G(\boldsymbol{x},\boldsymbol{y}) > 0 \end{cases}. \tag{7}$$

3. PROPOSED METHOD

In this section, a fully decoupled approach for HRA-RI is developed. Based on the ALPI method (Dang et al. (2021, 2022b)), the posterior mean and the upper bound of posterior variance of FPF are firstly derived. Second, a two-stage active learning strategy is proposed to obtain new points. Furthermore, in order to achieve a sufficient level of accuracy for the failure probability estimate, sequential MCS is applied in this method.

3.1. From prior to posterior

In engineering practice, the real response of performance function can be obtained only after evaluating $G(\boldsymbol{x},\boldsymbol{y})$. Nevertheless, it is intractable to obtain the response at every point because the evaluation is usually laborious. According to Bayes' theorem, based on the prior information about $G(\boldsymbol{x},\boldsymbol{y})$, the associated posterior distribution can be deduced. For brevity and convenience, in the following sections, the hybrid variable is denoted as $\boldsymbol{U} = (\boldsymbol{X},\boldsymbol{Y})$, where $\boldsymbol{u} = (\boldsymbol{x},\boldsymbol{y})$ is a realization. The details are described as follows.

To start with, let us assign a Gaussian process (GP) over $G(\boldsymbol{u})$ as a prior, which is expressed as:

$$\hat{G}_{pr} \sim GP(m_{pr}(\boldsymbol{u}), c_{pr}(\boldsymbol{u},\boldsymbol{u}')), \tag{8}$$

where $\hat{G}_{pr}$ is the prior distribution of $G(\boldsymbol{u})$, $m_{pr}(\boldsymbol{u})$ and $c_{pr}(\boldsymbol{u},\boldsymbol{u}')$ are the prior mean and the covariance functions with respect to two arbitrary points $\boldsymbol{u}$ and $\boldsymbol{u}'$, respectively. Without loss of generality, here $m_{pr}(\boldsymbol{u})$ is assumed to be a constant β, while the squared exponential kernel function is employed for $c_{pr}(\boldsymbol{u},\boldsymbol{u}')$:

$$m_{pr}(\boldsymbol{u}) = \beta, \tag{9}$$

$$c_{pr}(\boldsymbol{u},\boldsymbol{u}') = \sigma^2 \exp\left(-\sum_{k=1}^{d} \frac{(u_k - u_k')^2}{2\ell_k^2}\right), \tag{10}$$

where σ^2 is the process variance, ℓ_k is the kth element of the length scale vector $\boldsymbol{\ell}$, $d = n_{\boldsymbol{X}} + n_{\boldsymbol{Y}}$ denotes the dimension of uncertainty. Under this setting, the hyper-parameter $\boldsymbol{\vartheta} = [\beta, \sigma, \ell_1, \ell_2, \dots, \ell_d]$ remains to be identified. Let $\mathscr{U} = \left\{\boldsymbol{u}^{(i)}\right\}_{i=1}^{n}$ and $\mathscr{G} = \left\{G^{(i)} = G(\boldsymbol{u}^{(i)})\right\}_{i=1}^{n}$ denote an $n \times d$ matrix containing n sample points and an $n \times 1$ vector collecting the corresponding values of G function, respectively. Then, given n observations $\{\mathscr{U}, \mathscr{G}\}$, the maximum likelihood estimation (MLE) (Williams and Rasmussen (2006)) is adopted to determine the hyper-parameter $\boldsymbol{\vartheta}$.

After acquiring the hyper-parameter $\boldsymbol{\vartheta}$, the posterior distribution of $G(\boldsymbol{u})$ can be obtained:

$$\hat{G}_{po} \sim GP(m_{po}(\boldsymbol{u}), c_{po}(\boldsymbol{u},\boldsymbol{u}')), \tag{11}$$

where $m_{po}(\boldsymbol{u})$ and $c_{po}(\boldsymbol{u},\boldsymbol{u}')$ are the posterior mean and covariance functions, which are derived as follows:

$$\begin{aligned} m_{po}(\boldsymbol{u}) =& m_{pr}(\boldsymbol{u}) \\ &+ \boldsymbol{c}_{pr}^{\mathrm{T}}(\boldsymbol{u},\mathscr{U}) \boldsymbol{C}_{pr}^{-1} (\mathscr{G} - \boldsymbol{m}_{pr}), \end{aligned} \tag{12}$$

$$\begin{aligned} c_{po}(\boldsymbol{u},\boldsymbol{u}') =& c_{pr}(\boldsymbol{u},\boldsymbol{u}') \\ &- \boldsymbol{c}_{pr}^{\mathrm{T}}(\boldsymbol{u},\mathscr{U}) \boldsymbol{C}_{pr}^{-1} \boldsymbol{c}_{pr}(\mathscr{U},\boldsymbol{u}'), \end{aligned} \tag{13}$$

where $\boldsymbol{c}_{pr}(\boldsymbol{u},\mathscr{U})$ is an $n \times 1$ covariance vector with ith element being $c_{pr}(\boldsymbol{u},\boldsymbol{u}^{(i)})$, $\boldsymbol{C}_{pr}$ denotes an $n \times n$ covariance matrix whose (i,j)th entry is $c_{pr}(\boldsymbol{u}^{(i)},\boldsymbol{u}^{(j)})$.

3.2. *Posterior information about failure probability*

It is worth noting that a Gaussian process prior gives rise to a posterior which is again a Gaussian process (Williams and Rasmussen (2006)). Accordingly, at any point $\boldsymbol{u} \notin \mathscr{U}$, the posterior distribution of the failure indicator $\hat{I}_F(\boldsymbol{u})$ is a Bernoulli random variable, of which mean and variance functions are (Dang et al. (2022a)):

$$m_{\hat{I}_F}(\boldsymbol{u}) = \Phi\left(\frac{-m_{po}(\boldsymbol{u})}{\sqrt{\sigma^2_{po}(\boldsymbol{u})}}\right), \tag{14}$$

$$\sigma^2_{\hat{I}_F}(\boldsymbol{u}) = \Phi\left(\frac{-m_{po}(\boldsymbol{u})}{\sqrt{\sigma^2_{po}(\boldsymbol{u})}}\right)\Phi\left(\frac{m_{po}(\boldsymbol{u})}{\sqrt{\sigma^2_{po}(\boldsymbol{u})}}\right), \tag{15}$$

where $\Phi(\cdot)$ denotes the cumulative distribution function (CDF) of the standard normal variable, $\sigma^2_{po}(\boldsymbol{u})$ is the posterior variance function of $G(\boldsymbol{u})$.

It should be pointed out that the sample point $\boldsymbol{u}$ herein includes random and interval samples (i.e., $\hat{I}_F(\boldsymbol{u}) = \hat{I}_F(\boldsymbol{x},\boldsymbol{y})$). In this case, the FPF with respect to interval variables (denoted as $\hat{P}_f(\boldsymbol{y})$) is a stochastic process. That is, at arbitrary point $\boldsymbol{y}^\star$, the failure probability $\hat{P}_f$ is a random variable, whose posterior mean can be derived as:

$$\begin{aligned} m_{\hat{P}_f}(\boldsymbol{y}^\star) &= \mathbb{E}\left[\int_{\mathbb{X}} \hat{I}_F(\boldsymbol{x},\boldsymbol{y}^\star) f_{\boldsymbol{X}}(\boldsymbol{x})\mathrm{d}\boldsymbol{x}\right] \\ &= \int_{\mathbb{X}} m_{\hat{I}_F}(\boldsymbol{x},\boldsymbol{y}^\star) f_{\boldsymbol{X}}(\boldsymbol{x})\mathrm{d}\boldsymbol{x} \\ &= \mathbb{E}_{\mathbb{X}}\left[\Phi\left(\frac{-m_{po}(\boldsymbol{x},\boldsymbol{y}^\star)}{\sqrt{\sigma^2_{po}(\boldsymbol{x},\boldsymbol{y}^\star)}}\right)\right], \end{aligned} \tag{16}$$

where $\mathbb{E}[\cdot]$ denotes the posterior expectation operator, $\mathbb{E}_{\mathbb{X}}[\cdot]$ is the expectation operator with respect to $\boldsymbol{x}$. Furthermore, the corresponding posterior variance of failure probability can be expressed as:

$$\begin{aligned} &\sigma^2_{\hat{P}_f}(\boldsymbol{y}^\star) \\ &= \mathbb{E}\left[\left(\hat{P}_f(\boldsymbol{y}^\star) - m_{\hat{P}_f}(\boldsymbol{y}^\star)\right)^2\right] \\ &= \int_{\mathbb{X}}\int_{\mathbb{X}} \mathrm{cov}\left(\hat{I}_F(\boldsymbol{x},\boldsymbol{y}^\star), \hat{I}_F(\boldsymbol{x}',\boldsymbol{y}^\star)\right) \\ &\qquad f_{\boldsymbol{X}}(\boldsymbol{x}) f_{\boldsymbol{X}}(\boldsymbol{x}')\mathrm{d}\boldsymbol{x}\mathrm{d}\boldsymbol{x}', \end{aligned} \tag{17}$$

where $\mathrm{cov}\left(\hat{I}_F(\boldsymbol{x},\boldsymbol{y}^\star), \hat{I}_F(\boldsymbol{x}',\boldsymbol{y}^\star)\right)$ denotes the posterior covariance between $\hat{I}_F(\boldsymbol{x},\boldsymbol{y}^\star)$ and $\hat{I}_F(\boldsymbol{x}',\boldsymbol{y}^\star)$. For convenience of numerical implementation, the upper bound of the posterior variance is adopted herein. According to the covariance inequality, the upper bound of $\sigma^2_{\hat{P}_f}(\boldsymbol{y}^\star)$ is deduced as:

$$\begin{aligned} \sigma^2_{\hat{P}_f}(\boldsymbol{y}^\star) &= \int_{\mathbb{X}}\int_{\mathbb{X}} \mathrm{cov}\left(\hat{I}_F(\boldsymbol{x},\boldsymbol{y}^\star), \hat{I}_F(\boldsymbol{x}',\boldsymbol{y}^\star)\right) \\ &\qquad f_{\boldsymbol{X}}(\boldsymbol{x}) f_{\boldsymbol{X}}(\boldsymbol{x}')\mathrm{d}\boldsymbol{x}\mathrm{d}\boldsymbol{x}' \\ &\le \int_{\mathbb{X}}\int_{\mathbb{X}} \sqrt{\sigma^2_{\hat{I}_F}(\boldsymbol{x},\boldsymbol{y}^\star)}\sqrt{\sigma^2_{\hat{I}_F}(\boldsymbol{x}',\boldsymbol{y}^\star)} \\ &\qquad f_{\boldsymbol{X}}(\boldsymbol{x}) f_{\boldsymbol{X}}(\boldsymbol{x}')\mathrm{d}\boldsymbol{x}\mathrm{d}\boldsymbol{x}' \\ &= \left(\int_{\mathbb{X}} \sqrt{\sigma^2_{\hat{I}_F}(\boldsymbol{x},\boldsymbol{y}^\star)} f_{\boldsymbol{X}}(\boldsymbol{x})\mathrm{d}\boldsymbol{x}\right)^2 \\ &= \left(\mathbb{E}_{\mathbb{X}}[\sqrt{\sigma^2_{\hat{I}_F}(\boldsymbol{x},\boldsymbol{y}^\star)}]\right)^2 = \overline{\sigma^2_{\hat{P}_f}}(\boldsymbol{y}^\star), \end{aligned} \tag{18}$$

In this method, $m_{\hat{P}_f}(\boldsymbol{y}^\star)$ is used to approximate the actual failure probability, while $\overline{\sigma^2_{\hat{P}_f}}(\boldsymbol{y}^\star)$ can be used as a measure of the maximum epistemic uncertainty.

3.3. *A two-stage adaptive Bayesian active learning strategy*

In order to improve the efficiency of proposed method, a two-stage adaptive Bayesian active learning strategy is introduced in the followings.

At the beginning of Bayesian active learning, the posterior mean function of failure probability will deviate significantly from the true one. This means that the extreme values of the current failure probability function (i.e., the interval of failure probability) are not reliable. In this regard, a global failure probability (denoted as $\hat{P}_{f,g}$) which is a random variable is introduced in the first stage. Similar to Eq. (16), the posterior mean of $\hat{P}_{f,g}$ can be derived as:

$$\begin{aligned} m_{\hat{P}_{f,g}} &= \mathbb{E}\left[\hat{P}_{f,g}\right] \\ &= \int_{\mathbb{Y}} \mathbb{E}\left[\int_{\mathbb{X}} \hat{I}_F(\boldsymbol{x},\boldsymbol{y}) f_{\boldsymbol{X}}(\boldsymbol{x})\mathrm{d}\boldsymbol{x}\right]\mathrm{d}\boldsymbol{y} \\ &= \int_{\mathbb{Y}} \mathbb{E}_{\mathbb{X}}\left[\Phi\left(\frac{-m_{po}(\boldsymbol{x},\boldsymbol{y})}{\sqrt{\sigma^2_{po}(\boldsymbol{x},\boldsymbol{y})}}\right)\right]\mathrm{d}\boldsymbol{y}. \end{aligned} \tag{19}$$

Similar to Eqs. (17) and (18), the upper bound of the posterior variance of $\hat{P}_{f,g}$ is expressed as:

$$\begin{aligned}
&\sigma^2_{\hat{P}_{f,g}} \\
&=\int_{\mathbb{X}}\int_{\mathbb{X}}\int_{\mathbb{Y}}\int_{\mathbb{Y}} \operatorname{cov}\left(\hat{I}_F(\boldsymbol{x},\boldsymbol{y}),\hat{I}_F(\boldsymbol{x}',\boldsymbol{y}')\right) \\
&\qquad f_{\boldsymbol{X}}(\boldsymbol{x}) f_{\boldsymbol{X}}(\boldsymbol{x}')\mathrm{d}\boldsymbol{x}\mathrm{d}\boldsymbol{x}'\mathrm{d}\boldsymbol{y}\mathrm{d}\boldsymbol{y}' \\
&\le \int_{\mathbb{X}}\int_{\mathbb{X}}\int_{\mathbb{Y}}\int_{\mathbb{Y}} \sqrt{\sigma^2_{\hat{I}_F}(\boldsymbol{x},\boldsymbol{y})}\sqrt{\sigma^2_{\hat{I}_F}(\boldsymbol{x}',\boldsymbol{y}')} \\
&\qquad f_{\boldsymbol{X}}(\boldsymbol{x}) f_{\boldsymbol{X}}(\boldsymbol{x}')\mathrm{d}\boldsymbol{x}\mathrm{d}\boldsymbol{x}'\mathrm{d}\boldsymbol{y}\mathrm{d}\boldsymbol{y}' \\
&=\left(\int_{\mathbb{Y}} \mathbb{E}_{\mathbb{X}}\left[\sqrt{\Phi\left(\frac{-m_{po}(\boldsymbol{x},\boldsymbol{y})}{\sqrt{\sigma^2_{po}(\boldsymbol{x},\boldsymbol{y})}}\right)}\right.\right. \\
&\qquad \left.\left.\times\sqrt{\Phi\left(\frac{m_{po}(\boldsymbol{x},\boldsymbol{y})}{\sqrt{\sigma^2_{po}(\boldsymbol{x},\boldsymbol{y})}}\right)}\right]\mathrm{d}\boldsymbol{y}\right)^2 \\
&=\overline{\sigma^2_{\hat{P}_{f,g}}},
\end{aligned} \tag{20}$$

where $\mathbb{E}_{\mathbb{XY}}$ denotes expectation operator with respect to $\boldsymbol{x}$ and $\boldsymbol{y}$. Actually, $\hat{P}_{f,g}$ can be intuitively interpreted as the integral of $\hat{P}_f(\boldsymbol{y})$ with respect to $\boldsymbol{y}$, and its posterior mean $m_{\hat{P}_{f,g}}$ can be used to reflect the global accuracy of $\hat{P}_f(\boldsymbol{y})$ to some degree, while $\overline{\sigma^2_{\hat{P}_{f,g}}}$ can measure the epistemic uncertainty. After the global accuracy of $\hat{P}_f(\boldsymbol{y})$ is satisfied in the first stage, the lower and upper bounds of failure probability can be determined efficiently in the second stage.

In order to update the posterior information, two active learning functions are proposed to identify update points in each stage. Based on Eqs. (20) and (18), an active learning function called global uncertainty contribution (GUC) for the first stage is defined as:

$$\begin{aligned}
\mathrm{GUC}(\boldsymbol{u}) = &\sqrt{\Phi\left(\frac{-m_{po}(\boldsymbol{u})}{\sqrt{\sigma^2_{po}(\boldsymbol{u})}}\right)\Phi\left(\frac{m_{po}(\boldsymbol{u})}{\sqrt{\sigma^2_{po}(\boldsymbol{u})}}\right)} \\
&\times f_{\boldsymbol{X}}(\boldsymbol{x}),
\end{aligned} \tag{21}$$

while another function called local uncertainty contribution (LUC) for the second stage is defined as:

$$\begin{aligned}
\mathrm{LUC}(\boldsymbol{x},\boldsymbol{y}^{opt}) = &\sqrt{\Phi\left(\frac{-m_{po}(\boldsymbol{x},\boldsymbol{y}^{opt})}{\sqrt{\sigma^2_{po}(\boldsymbol{x},\boldsymbol{y}^{opt})}}\right)} \\
&\sqrt{\Phi\left(\frac{m_{po}(\boldsymbol{x},\boldsymbol{y}^{opt})}{\sqrt{\sigma^2_{po}(\boldsymbol{x},\boldsymbol{y}^{opt})}}\right)} \times f_{\boldsymbol{X}}(\boldsymbol{x}),
\end{aligned} \tag{22}$$

where $\boldsymbol{y}^{opt}$ is the global maximum point (or minimum point) of the posterior mean function in Eq. (16). It should be noted that in the first stage, a point $\boldsymbol{u}$ with the maximum value of GUC is selected in each iteration, while a point $\boldsymbol{x}$ with the maximum value of LUC is chosen in the second stage. Furthermore, $\boldsymbol{y}^{opt}$ is obtained by maximizing the function in Eq. (16) when estimate the upper bound of $\hat{P}_f$, while $\boldsymbol{y}^{opt}$ is obtained by minimizing Eq. (16) when estimate the lower bound of $\hat{P}_f$.

Based on the upper bound of posterior coefficient of variation of $\hat{P}_{f,g}$ and $\hat{P}_f$, herein two stopping criteria are introduced for the first and second stages, respectively:

$$\delta(\hat{P}_{f,g}) = \frac{\sqrt{\overline{\sigma^2_{\hat{P}_{f,g}}}}}{m_{\hat{P}_{f,g}}}, \tag{23}$$

$$\delta(\hat{P}_f) = \frac{\sqrt{\overline{\sigma^2_{\hat{P}_f}}(\boldsymbol{y}^{opt})}}{m_{\hat{P}_f}(\boldsymbol{y}^{opt})}. \tag{24}$$

Note that numerical analysis is still required to obtain the posterior mean values $m_{\hat{P}_{f,g}}$, $m_{\hat{P}_f}(\boldsymbol{y}^{opt})$ and the upper bounds of posterior variance $\overline{\sigma^2_{\hat{P}_{f,g}}}$, $\overline{\sigma^2_{\hat{P}_f}}(\boldsymbol{y}^{opt})$ which are analytically intractable. In this study, the sequential MCS is employed as a numerical method for estimation in both stages.

3.4. Procedure of the proposed method

The complete procedure of the proposed method is elaborated in below, where the first stage consists of Step 2 $\sim$ 5 and the second stage consists of Step 6 $\sim$ 10.

Step 1: Define initial design of experiments (DoE). In this work, Latin Hypercube Sampling

(LHS) is employed to produce training points uniformly to construct a GP model.

Step 2: Apply sequential MCS to determine the number of sample points. MCS is used to generate N_Ω sample points first, and the set of points is denoted as Ω. Then, calculate the coefficient of variation of $m_{\hat{P}_{f,g}}$ and $\sqrt{\overline{\sigma^2_{\hat{P}_{f,g}}}}$ (denoted as CV_1 and CV_2) according to the bias of an estimator:

$$CV_1 = \frac{\sqrt{\frac{1}{N_\Omega(N_\Omega-1)}\sum_{i=1}^{N_\Omega}\left(S_i-\overline{S}\right)^2}}{\frac{1}{N_\Omega}\sum_{i=1}^{N_\Omega}S_i}, \tag{25}$$

$$CV_2 = \frac{\sqrt{\frac{1}{N_\Omega(N_\Omega-1)}\sum_{i=1}^{N_\Omega}\left(S_i^\star-\overline{S^\star}\right)^2}}{\frac{1}{N_\Omega}\sum_{i=1}^{N_\Omega}S_i^\star}, \tag{26}$$

where S_i and $S_i^\star$ are defined as:

$$S_i = \Phi\left(\frac{-m_{po}(\boldsymbol{u}_i)}{\sqrt{\sigma^2_{po}(\boldsymbol{u}_i)}}\right),\ i=1,2,...,N_\Omega, \tag{27}$$

$$S_i^\star = \sqrt{\Phi\left(\frac{-m_{po}(\boldsymbol{u}_i)}{\sqrt{\sigma^2_{po}(\boldsymbol{u}_i)}}\right)\Phi\left(\frac{m_{po}(\boldsymbol{u}_i)}{\sqrt{\sigma^2_{po}(\boldsymbol{u}_i)}}\right)}, \tag{28}$$

$\overline{S}$ and $\overline{S^\star}$ are the corresponding mean values, respectively.

Step 3: Judge the stopping criterion of adaptive MCS. If $CV_1 \le \varepsilon_1$ and $CV_2 \le \varepsilon_2$, go to Step 4. Otherwise, generate N_Ω new points and add them into Ω, then calculate CV_1 and CV_2 again until the stopping criterion is satisfied. ε_1 and ε_2 are set to be 0.01.

Step 4: Check the stopping criterion of GP model updating. In this stage, Eq. (23) is adopted to assess the accuracy of failure probability estimate. If $\delta(\hat{P}_{f,g}) \le 0.01$, go to Step 6.

Step 5: Select a now point from Ω by GUC and evaluate the $G(\boldsymbol{X},\boldsymbol{Y})$ at this point. Add the new point and the response into observations to update GP model, then go back to Step 4.

Step 6: Generate $N_{\Omega'}$ new sample points by MCS denoted as Ω'.

Step 7: Identify the global maximum point $\boldsymbol{y}^{opt}$ (or minimum point) by solving an optimization problem. Then, calculate the coefficient of variation of $m_{\hat{P}_f}(\boldsymbol{y}^{opt})$ and $\sqrt{\overline{\sigma^2_{\hat{P}_f}}(\boldsymbol{y}^{opt})}$ (denoted as CV_3 and CV_4):

$$CV_3 = \frac{\sqrt{\frac{1}{N_{\Omega'}(N_{\Omega'}-1)}\sum_{i=1}^{N_{\Omega'}}\left(S_i(\boldsymbol{y}^{opt})-\overline{S(\boldsymbol{y}^{opt})}\right)^2}}{\frac{1}{N_{\Omega'}}\sum_{i=1}^{N_{\Omega'}}S_i(\boldsymbol{y}^{opt})}, \tag{29}$$

$$CV_4 = \frac{\sqrt{\frac{1}{N_{\Omega'}(N_{\Omega'}-1)}\sum_{i=1}^{N_{\Omega'}}\left(S_i^\star(\boldsymbol{y}^{opt})-\overline{S^\star(\boldsymbol{y}^{opt})}\right)^2}}{\frac{1}{N_{\Omega'}}\sum_{i=1}^{N_{\Omega'}}S_i^\star(\boldsymbol{y}^{opt})}, \tag{30}$$

where $S_i(\boldsymbol{y}^{opt})$ and $S_i^\star(\boldsymbol{y}^{opt})$ are defined as:

$$S_i(\boldsymbol{y}^{opt}) = \Phi\left(\frac{-m_{po}(\boldsymbol{x}_i,\boldsymbol{y}^{opt})}{\sqrt{\sigma^2_{po}(\boldsymbol{x}_i,\boldsymbol{y}^{opt})}}\right),\ i=1,2,...,N_{\Omega'}, \tag{31}$$

$$\begin{aligned} S_i^\star(\boldsymbol{y}^{opt}) = &\sqrt{\Phi\left(\frac{-m_{po}(\boldsymbol{x}_i,\boldsymbol{y}^{opt})}{\sqrt{\sigma^2_{po}(\boldsymbol{x}_i,\boldsymbol{y}^{opt})}}\right)} \\ &\times\sqrt{\Phi\left(\frac{m_{po}(\boldsymbol{x}_i,\boldsymbol{y}^{opt})}{\sqrt{\sigma^2_{po}(\boldsymbol{x}_i,\boldsymbol{y}^{opt})}}\right)}. \end{aligned} \tag{32}$$

$\overline{S(\boldsymbol{y}^{opt})}$ and $\overline{S^\star(\boldsymbol{y}^{opt})}$ are the corresponding mean values, respectively.

Step 8: Check the termination criterion. If $CV_3 \le \varepsilon_3$ and $CV_4 \le \varepsilon_4$, go to Step 9. Otherwise, generate $N_{\Omega'}$ new points and add them into Ω', then go back to Step 7. In this work, ε_3 and ε_4 are set to be 0.01.

Step 9: Judgement of the stopping criterion of GP model updating. If $\delta(\hat{P}_f) \le 0.01$, the procedure will be stopped and the upper bound (or lower bound) of the failure probability is obtained. Otherwise, identify a new $\boldsymbol{y}^{opt}$ by using optimization algorithm.

Step 10: Select a new point from Ω' using LUC. Add the new point and the response into observations to update GP model, then go back to Step 9.

4. NUMERICAL EXAMPLE

In this example, the performance function is described below (Yang et al. (2015)):

$$G(\boldsymbol{X}, y) = \sin\left(\frac{5X_1}{2}\right) - \frac{(X_1^2+4)(X_2-1)}{20} + y, \tag{33}$$

where $\boldsymbol{X} = (X_1, X_2)^{\mathrm{T}}$ denotes the vector of independent normal distributed random variables, and $X_1 \sim N(1.5, 1^2), X_2 \sim N(2.5, 1^2)$; y represents the interval variable and $y \in [2, 2.5]$.

First, 10 training points are generated to construct an initial GP model. Then, sequential MCS is performed and N is set to be 10^5. New training points selected in the two stages are shown in Figure 1. It can be seen in Figure 1, most new points are located in the vicinity of limit state where the response of performance function is zero. Furthermore, the majority of these points are identified in the first stage, while only a few points are chosen in the second stage. This illustrates that larger epistemic uncertainties exist in estimating the global failure probability $\hat{P}_{f,g}$, and more points are required. After the global trend of failure probability is accurate enough, a minority of new points are chosen to refine the local trend of failure probability function in the second stage.

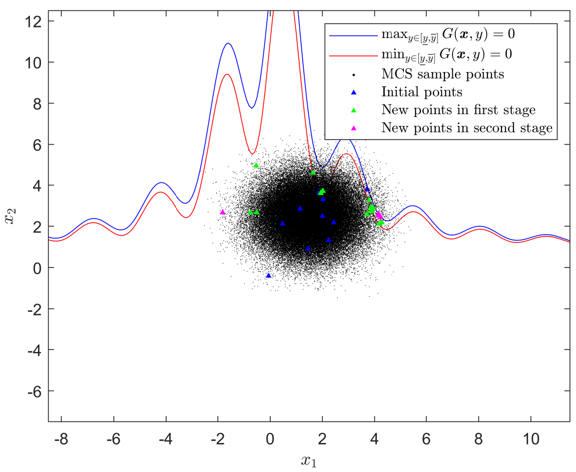

Figure 1: New points in Example 1

Figure 2 displays the curve of failure probability with respect to y in one independent run. It can be seen that the curve of failure probability is very close to the reference curve obtained by MCS.

Table 1 summarizes comparative results where relative errors for bounds of failure probability are 0.17% and 0.19% via the proposed method, and 34 performance function calls are required in the proposed method. Accordingly, this method can estimate bounds of failure probability efficiently and accurately.

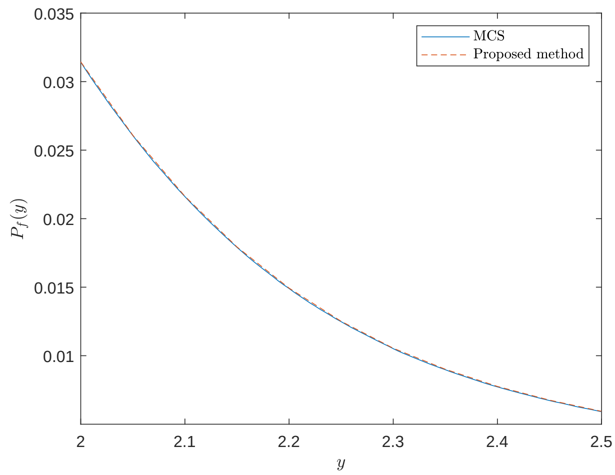

Figure 2: Curve of failure probability function

Table 1: Comparative results in Example 1.

Methods	P_f^L	$error(P_f^L)$	P_f^U	$error(P_f^U)$	Function calls
MCS	5.910‰	–	31.32‰	–	100×10^5
FORM-UUA	5.868‰	0.71%	8.814‰	71.86%	25+878=903
ALK-HRA	5.829‰	1.37%	31.46‰	0.45%	54
Proposed method	5.900‰	0.17%	31.26‰	0.19%	34

5. CONCLUSIONS

This paper presents a fully decoupled approach for HRA-RI. In this method, the posterior expectation function and the upper bound of the posterior variance function of FPF are derived based on Bayes' theorem. In addition, a two-stage adaptive active learning strategy is developed, where two learning functions are defined based on the upper bound of posterior variance of $\hat{P}_{f,g}$ and $\hat{P}_f$. One example is investigated to demonstrate the advantages of the proposed method. Results indicate that the proposed method can produce more accurate lower and upper bounds of failure probability, while function calls are less than MCS, FORM-UUA, and ALK-HRA. Moreover, this method can provide the lower and upper bounds of failure probability and a satisfying global estimation of FPF as well.

ACKNOWLEDGMENT

Jinxing Liu and Chao Dang are grateful to the support from China Scholarship Council (CSC).

6. REFERENCES

Beer, M., Ferson, S., and Kreinovich, V. (2013a). "Imprecise probabilities in engineering analyses." *Mechanical Systems and Signal Processing*, 37(1-2), 4–29.

Beer, M., Zhang, Y., Quek, S. T., and Phoon, K. K. (2013b). "Reliability analysis with scarce information: Comparing alternative approaches in a geotechnical engineering context." *Structural Safety*, 41, 1–10.

Brevault, L., Lacaze, S., Balesdent, M., and Missoum, S. (2016). "Reliability analysis in the presence of aleatory and epistemic uncertainties, application to the prediction of a launch vehicle fallout zone." *Journal of Mechanical Design*, 138(11), 111401.

Dang, C., Valdebenito, M. A., Faes, M. G., Wei, P., and Beer, M. (2022a). "Structural reliability analysis: A Bayesian perspective." *Structural Safety*, 99, 102259.

Dang, C., Wei, P., Faes, M. G., Valdebenito, M. A., and Beer, M. (2022b). "Parallel adaptive bayesian quadrature for rare event estimation." *Reliability Engineering & System Safety*, 225, 108621.

Dang, C., Wei, P., Song, J., and Beer, M. (2021). "Estimation of failure probability function under imprecise probabilities by active learning–augmented probabilistic integration." *ASCE-ASME Journal of Risk and Uncertainty in Engineering Systems, Part A: Civil Engineering*, 7(4), 04021054.

Der Kiureghian, A. and Ditlevsen, O. (2009). "Aleatory or epistemic? Does it matter?." *Structural Safety*, 31(2), 105–112.

Helton, J. C. and Burmaster, D. E. (1996). "Guest editorial: treatment of aleatory and epistemic uncertainty in performance assessments for complex systems." *Reliability Engineering & System Safety*, 54(2-3), 91–94.

Hong, L., Li, H., Gao, N., Fu, J., and Peng, K. (2021). "Random and multi-super-ellipsoidal variables hybrid reliability analysis based on a novel active learning kriging model." *Computer Methods in Applied Mechanics and Engineering*, 373, 113555.

Huang, B. and Du, X. (2008). "Probabilistic uncertainty analysis by mean-value first order saddlepoint approximation." *Reliability Engineering & System Safety*, 93(2), 325–336.

Jiang, C., Zhang, Z., Han, X., and Liu, J. (2013). "A novel evidence-theory-based reliability analysis method for structures with epistemic uncertainty." *Computers & Structures*, 129, 1–12.

Luo, Y., Kang, Z., and Li, A. (2009). "Structural reliability assessment based on probability and convex set mixed model." *Computers & Structures*, 87(21-22), 1408–1415.

Williams, C. K. and Rasmussen, C. E. (2006). *Gaussian processes for machine learning*, Vol. 2. MIT press Cambridge, MA.

X. Du (2008). "Unified uncertainty analysis by the first order reliability method." *Journal of Mechanical Design*, 130(9) 091401.

Xiao, N.-C., Huang, H.-Z., Wang, Z., Liu, Y., and Zhang, X.-L. (2012). "Unified uncertainty analysis by the mean value first order saddlepoint approximation." *Structural and Multidisciplinary Optimization*, 46(6), 803–812.

Yang, X., Liu, Y., Gao, Y., Zhang, Y., and Gao, Z. (2015). "An active learning kriging model for hybrid reliability analysis with both random and interval variables." *Structural and Multidisciplinary Optimization*, 51(5), 1003–1016.

Zhang, J., Xiao, M., Gao, L., and Fu, J. (2018). "A novel projection outline based active learning method and its combination with kriging metamodel for hybrid reliability analysis with random and interval variables." *Computer Methods in Applied Mechanics and Engineering*, 341, 32–52.